

Quark form factors and leading double logarithms in quantum chromodynamics

S. D. Ellis and W. J. Stirling

Department of Physics, University of Washington, Seattle, Washington 98195

(Received 5 June 1980)

Perturbative quantum-chromodynamic corrections involving the emission of gluons which are both soft and collinear are discussed for both hadronic production of lepton pairs and e^+e^- annihilation. The result is an exponential, double-logarithmic quark "form factor." The differences between previous analyses are clarified and the possible experimental observation of the form factor is discussed and illustrated.

I. INTRODUCTION

For many processes involving hadrons it is a remarkably good first approximation to view the hadrons as composed of essentially pointlike, non-interacting quarks. Such processes are characterized in phase space by a limit where all relevant variables are becoming large together, e.g., fixed-angle inclusive scattering. This simple description of such hadronic processes is generically referred to as the parton model.¹ It can be shown² that the general factorized picture of these interactions central to the parton model survives in the context of quantum chromodynamics (QCD)³, the candidate theory describing the interactions between the quarks themselves. This is a non-trivial result. It depends first on the asymptotic smallness of the effective coupling at scale Q^2 given by

$$\alpha_s(Q^2) = \frac{g^2}{4\pi} \simeq \frac{12\pi}{(33 - 2N_f)\ln(Q^2/\Lambda^2)} \equiv \frac{b}{\ln(Q^2/\Lambda^2)}, \quad (1.1)$$

where N_f is the number of quark flavors and Λ^2 is essentially the scale where the coupling is large, determined phenomenologically to be of order $(500 \text{ MeV}/c)^2$. It also depends on the fact that the logarithmic singularities inherent in the theory can be factored in such a way as to associate them with the (renormalized) asymptotic wave functions of presumably confined quarks inside hadrons. As a result, these quark distributions within hadrons depend on the resolution scale, Q^2 , with which the quarks are observed. The singularities arise in perturbation theory, much as in QED, from the emission of the massless gauge particles, the gluons. An example is illustrated in Fig. 1, which is to be considered as a piece of a Feynman graph. The quark of momentum $p - k$ can be close to the mass shell and hence yield a logarithmic singularity both when $k_\mu \rightarrow 0$, an infrared singularity, and, to the extent the quarks are massless, when the gluon is collinear with the quark. The $(\log)^2$ singularity which arises from the overlap of

these regions is characteristic of vector theories.

The next step is to calculate the nonsingular perturbative corrections to the simple parton picture. Again care must be taken to avoid the re-appearance of the mass singularities mentioned above. Considerable progress⁴ has been made both in the phenomenological understanding of the structure of the theory and in the direction of defining precise experimental tests. The simplest perturbative results are, however, confined to processes characterized by a single large invariant Q^2 , with all relevant scattering angles large and fixed. Examples of such processes are total e^+e^- annihilation into hadrons and hadronic production of large-mass lepton pairs (the Drell-Yan process) either at very large transverse momenta $Q_T^2 \approx Q^2$ or integrated over transverse momenta.

There has been considerable interest⁵⁻⁷ in extending the perturbative analysis into kinematic regions where there are two large invariants which nevertheless have a large ratio, corresponding to some angle becoming small. Such efforts, by enlarging the region of phenomenological applicability of the analysis, enhance one's ability to test QCD. Specific examples of such a kinematic regime are the measurement of Drell-Yan lepton pairs with $\Lambda^2 \ll Q_T^2 \ll Q^2$ and the measurement in e^+e^- annihilation of energy-energy correlations⁸ with two "calorimeters" which are nearly back to back. In these cases the footprints of the mass singularities reappear. At each order in perturbation theory the dominant corrections to the naive lepton-pair process are of the form $\alpha_s^n \ln^n(Q^2/Q_T^2)$ arising from the emission of n soft and collinear gluons. Thus for a sufficiently large ratio Q^2/Q_T^2 the perturbative approach breaks down

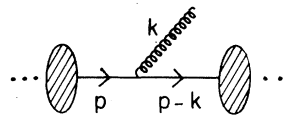


FIG. 1. Gluon emission from an internal line in a Feynman graph.

and it becomes necessary to treat the double-leading-logarithm approximation (DLLA) to all orders. An extremely attractive possibility is that these double-logarithmic terms exponentiate, much as in QED,⁹ leading to a vanishing rate in the limit $Q^2/Q_T^2 \rightarrow \infty$. It is to this topic that the following paper is addressed. The differences between the previous analyses⁵⁻⁷ will be clarified and the discussion extended to include the next-to-leading logarithms. Particular attention will be paid to the possibility of phenomenological application, i.e., observation, of these effects.

II. LARGE-MASS LEPTON PAIRS: FIRST ORDER

As an explicit example of the situation discussed above, consider the hadronic production of a massive photon (i.e., lepton pair of large total mass) via quark-antiquark annihilation. (The possibility of gluon-initiated processes is ignored in the present discussion for simplicity. A similar analysis for the gluon case could be carried out but the one given here is presumably adequate for pions and antiprotons on nucleon targets.) In the parton model this is viewed as in Fig. 2 and, in the limit $s = (p_A + p_B)^2 \rightarrow \infty$ with $Q^2/s = \tau$ fixed, the cross section is given by

$$\frac{d\sigma}{dQ^2} = \frac{4\pi\alpha^2}{9sQ^2} \int_0^1 dx_1 dx_2 \delta(x_1 x_2 - \tau) \times [G_{q/A}(x_1)G_{\bar{q}/B}(x_2) + A \leftrightarrow B]. \quad (2.1)$$

Here $G_{q/A}(x_1)$ is the distribution of quarks in hadron A with momentum fraction x_1 . When QCD perturbative corrections are included it is observed² that at order α_s^n there is an n -fold logarithmic divergence due to collinear emission of gluons, while the soft infrared singularities cancel between real- and virtual-gluon corrections. As mentioned earlier these divergences can be organized to all orders so as to be included in the definition of the renormalized, Q^2 -dependent distribution functions. Hence in the leading-single-logarithm approximation, i.e., keeping only the

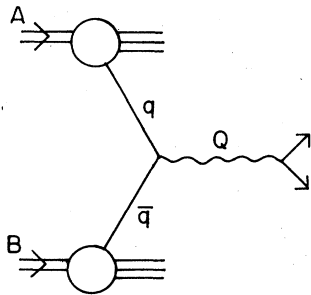


FIG. 2. Drell-Yan mechanism for large-mass lepton-pair production in hadronic collisions.

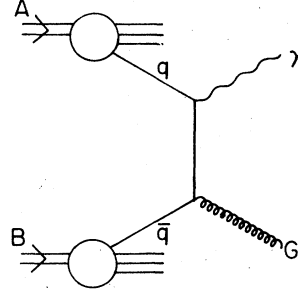


FIG. 3. Lowest-order diagram for the production of a virtual photon with large transverse momentum.

$\alpha_s^n \ln^n Q^2$ terms, $G(x)$ is replaced by $G(x, Q^2)$ (with an overall factor of $\frac{1}{3}$ to account for the average over the incident quark color).

Now consider the case wherein the transverse momentum is sufficiently large, $Q^2 \sim Q_T^2 \gg \Lambda^2$, so that the distribution of "intrinsic" transverse momenta of the quarks within the incident hadrons can be ignored. Then in "lowest-order" perturbation theory the dominant diagram is shown in Fig. 3 where the single gluon which balances the large Q_T is displayed and the infinity of collinear gluons contributing to the Q^2 -dependent distribution functions is implicit. The cross section assumes the form

$$\frac{d\sigma}{dQ^2 dQ_T^2} \sim \frac{4\pi\alpha^2}{9sQ^2} \int dx_1 dx_2 \times [G_{q/A}(x_1, Q^2)G_{\bar{q}/B}(x_2, Q^2) + A \leftrightarrow B] \times \hat{\sigma}(x_1, x_2, Q_T^2/s, Q^2/s), \quad (2.2)$$

where $\hat{\sigma}$ describes the central $2 \rightarrow 2$ process ($q + \bar{q} \rightarrow \gamma^* + G$)

$$\hat{\sigma} = \frac{\alpha_s C_F}{2\pi} \int d\hat{u} d\hat{t} \delta(\hat{u}\hat{t} - Q_T^2 \hat{s}) \delta(\hat{s} + \hat{t} + \hat{u} - Q^2) \times \left[\frac{(\hat{s} + \hat{t})^2 + (\hat{s} + \hat{u})^2}{\hat{t}\hat{u}} \right]. \quad (2.3)$$

The variables \hat{s} , \hat{t} , \hat{u} have the usual definitions, e.g., $\hat{t} = (q - Q)^2$, etc., and $C_F = \frac{4}{3}$ is the SU(3) Casimir operator value for the fundamental fer-

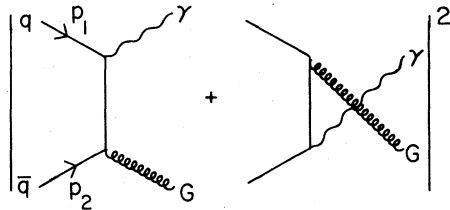


FIG. 4. Lowest-order subprocess diagrams for the production of a virtual photon with nonzero transverse momentum.

mion representation.

Finally, consider the limit $Q^2/Q_T^2 \gg 1$. Logarithms of this ratio appear from the integral over $\hat{\theta}$ and invalidate this lowest-order perturbative approach. To see this explicitly, focus now on the central hard process, the diagrams of Fig. 4, and ignore, for now, the complications due to the external hadrons. Parametrize the gluon momentum as

$$k = \theta p_2 + \mu p_1 + \vec{k}_T, \quad (2.4a)$$

where $\vec{k}_T \cdot p_1 = \vec{k}_T \cdot p_2 = 0$ and

$$\begin{aligned} \frac{d^3k}{2k_0} &= (p_1 \cdot p_2) d\theta d\mu d^2\vec{k}_T \delta\left(\theta\mu - \frac{k_T^2}{2p_1 \cdot p_2}\right) \\ &\equiv \frac{\hat{s}}{2} d\theta d\mu d^2\vec{k}_T \delta(\theta\mu - k_T^2/\hat{s}). \end{aligned} \quad (2.4b)$$

The cross section is given by ($\hat{\sigma}_0 = 4\pi\alpha^2/9\hat{s}$)

$$\begin{aligned} \frac{Q^2}{\hat{\sigma}_0} \frac{d^2\hat{\sigma}}{dQ^2 dQ_T^2} &= \int d\theta d\mu d^2\vec{k}_T \delta^{(2)}(\vec{k}_T + \vec{Q}_T) \delta(\theta\mu - \vec{k}_T^2/\hat{s}) \\ &\quad \times \delta(\hat{s}(1-\theta-\mu) - Q^2) \\ &\quad \times \frac{\alpha_s C_F}{2\pi} \frac{[(1-\theta)^2 + (1-\mu)^2]}{\theta\mu}, \end{aligned} \quad (2.5)$$

where all parton masses are zero. In order to isolate those (collinear) singularities which are to be associated with the external quark distributions it is useful to define moments in the form

$$F_n(Q_T^2/\hat{s}) = \int_0^{\hat{s}} dQ^2 \frac{d^2\hat{\sigma}}{dQ^2 dQ_T^2} \left(\frac{Q^2}{\hat{s}}\right)^{n+1}. \quad (2.6)$$

Then in the limit $Q_T^2/\hat{s} \ll 1$, F_n behaves as

$$F_n(Q_T^2/\hat{s}) \sim \frac{1}{Q_T^2} \int_{Q_T^2/\hat{s}} \frac{d\theta}{\theta} \sim \frac{1}{Q_T^2} \left(\ln \frac{\hat{s}}{Q_T^2} + C_n \right). \quad (2.7)$$

To explicitly exhibit the double logarithms characteristic of vector-boson theories define

$$\Sigma_n(p_T^2/\hat{s}) = \int_0^{p_T^2} dQ_T^2 F_n(Q_T^2/\hat{s}). \quad (2.8)$$

Since Eq. (2.8) includes also the region $Q_T = 0$ it is necessary both to regulate the inherent infrared singularities and to include the contribution of

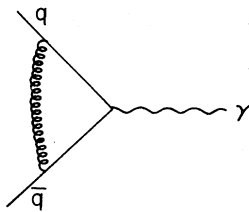


FIG. 5. One-virtual-gluon correction to the amplitude for $q\bar{q} \rightarrow \gamma$.

virtual gluons, e.g., Fig. 5, which is proportional to $\delta(Q_T^2)$. Various techniques are available to control the infrared singularities. In the present analysis it is sufficient to give the gluon a small mass λ^2 , which effectively replaces Q_T^2 by $Q_T^2 + \lambda^2$ in Eq. (2.7), but it is important to note that there can be subtleties involved in this choice.¹⁰

Returning to the real-emission graphs of Fig. 4 and assigning the gluons a mass λ^2 leads to a result of the form

$$\begin{aligned} \Sigma_{n,\alpha_s}^{\text{real}}(p_T^2/\hat{s}, \lambda^2/\hat{s}) \\ \sim \hat{\sigma}_0 \frac{\alpha_s C_F}{2\pi} \left[\ln^2 \frac{\hat{s}}{\lambda^2} + \left(\ln \frac{d_+}{d_-} \right) \left(\ln \frac{p_T^2}{\hat{s}} \right) \right. \\ \left. + (2a_n - 3) \left(\ln \frac{\hat{s}}{\lambda^2} - \ln \frac{d_+}{d_-} \right) + \dots \right], \end{aligned} \quad (2.9)$$

where the ellipsis refers to terms with no logarithm. The various symbols represent the quantities

$$d_{\pm} = \frac{1}{2} [1 \pm (1 - 4p_T^2/\hat{s})^{1/2}] \quad (2.10a)$$

and

$$a_n = \frac{3}{2} + \frac{1}{n+1} - \frac{1}{n+2} - 2 \sum_{i=1}^{n+1} \frac{1}{i}, \quad (2.10b)$$

where this last factor is the nonsinglet anomalous dimension familiar¹¹ from the study of the Q^2 dependence of the quark distribution functions. The corresponding virtual-gluon contribution is

$$\begin{aligned} \Sigma_{n,\alpha_s}^{\text{virtual}}\left(\frac{p_T^2}{\hat{s}}, \frac{\lambda^2}{\hat{s}}\right) \\ = \hat{\sigma}_0 \left[1 - \frac{\alpha_s C_F}{2\pi} \left(\ln^2 \frac{\hat{s}}{\lambda^2} - 3 \ln \frac{\hat{s}}{\lambda^2} \right) + \dots \right]. \end{aligned} \quad (2.11)$$

Thus to first order in α_s , which is taken as fixed for now,

$$\begin{aligned} \Sigma_{n,\alpha_s}\left(\frac{p_T^2}{\hat{s}}, \frac{\lambda^2}{\hat{s}}\right) = \hat{\sigma}_0 \left\{ 1 + \frac{\alpha_s C_F}{2\pi} \left[\ln \frac{d_+}{d_-} \left(3 + \ln \frac{p_T^2}{\hat{s}} \right) \right. \right. \\ \left. \left. + 2a_n \ln \frac{\hat{s} d_-}{\lambda^2 d_+} + \dots \right] \right\}. \end{aligned} \quad (2.12)$$

The limit $p_T^2 \rightarrow p_{T \text{ max}}^2 = \hat{s}/4$ ($d_{\pm} = \frac{1}{2}$) yields

$$\Sigma_{n,\alpha_s}\left(\frac{1}{4}, \frac{\lambda^2}{\hat{s}}\right) = \hat{\sigma}_0 \left[1 + \frac{\alpha_s C_F}{2\pi} (2a_n) \ln \frac{\hat{s}}{\lambda^2} + \dots \right], \quad (2.13)$$

where the 2 in the coefficient of a_n is the result of receiving one contribution from the quark distribution and one from the antiquark and is the $O(\alpha_s)$ version of the statement² of the factorization of the collinear singularities discussed above. In the opposite limit $p_T^2/\hat{s} \ll 1$, with $d_+ \approx 1$ and $d_- \approx p_T^2/\hat{s}$, the result is

$$\Sigma_{n,\alpha_s}\left(\frac{p_T^2}{\hat{s}}, \frac{\lambda^2}{\hat{s}}\right) = \hat{\sigma}_0 \left\{ 1 + \frac{\alpha_s C_F}{2\pi} \left[\ln \frac{\hat{s}}{p_T^2} \left(3 - \ln \frac{\hat{s}}{p_T^2} \right) + 2\alpha_n \ln \frac{p_T^2}{\lambda^2} + \dots \right] \right\} \quad (2.14a)$$

$$\underset{\text{DLLA}}{\simeq} \hat{\sigma}_0 \left[1 - \frac{\alpha_s C_F}{2\pi} \ln^2 \frac{\hat{s}}{p_T^2} + \dots \right], \quad (2.14b)$$

illustrating the double logarithms mentioned earlier. Note that in DLLA, the term which exhibits the coupled dependence on n and λ^2 drops out. The result in Eq. (2.14b) can be interpreted as an incomplete cancellation between the virtual-gluon contribution $(\alpha_s C_F/2\pi) \ln^2(\hat{s}/\lambda^2)$, and the real-gluon contribution $(\alpha_s C_F/2\pi) [\ln^2(\hat{s}/p_T^2) - \ln^2(\hat{s}/\lambda^2)]$, which is complete only in the limit $p_T^2 \rightarrow p_{T\text{max}}^2$.

It is interesting to digress for a moment to discuss the choice of gauge. While the form of the integrand in Eq. (2.5),

$$I(\theta, \mu) = \frac{(1-\theta)^2 + (1-\mu)^2}{\theta\mu}, \quad (2.15)$$

is independent of this choice, the contribution of specific diagrams and, in particular, the source of the double logarithm is gauge dependent. This is illustrated in Table I where the various real-emission diagrams (squared) and their contributions are displayed. The numbers in parentheses are the exponent of the logarithmic divergence for each individual graph. The results can be summarized by saying that in the axial and planar

gauges the leading double logarithms (and the leading number of collinear logarithms) arise from the ladder diagrams while the interference graphs give the leading contribution in Feynman gauge.

It should be clear (and will be demonstrated shortly) that the next order in perturbation theory will have contributions of the order $\alpha_s^2 \ln^4 \hat{s}/p_T^2$. Furthermore, it is easy to imagine kinematic regions where both $\alpha_s \ll 1$ and $\alpha_s \ln \hat{s}/p_T^2 < 1$ so that the DLLA is appropriate and yet $\alpha_s \ln^2 \hat{s}/p_T^2 > 1$ so that only an analysis to all orders is adequate. The most attractive possibility is that the sum to all orders of both real- and virtual-gluon emission simply results in an exponential form

$$\Sigma_{n,\text{all}}(p_T^2/\hat{s}) \underset{\text{DLLA}}{\simeq} \hat{\sigma}_0 \exp \left[-\frac{\alpha_s C_F}{2\pi} \ln^2(\hat{s}/p_T^2) \right] \quad (2.16)$$

in the double-leading-logarithm approximation. This is analogous to the situation in QED (Ref. 9) where forward processes are suppressed because of the divergent amplitudes to emit soft photons. While several analyses⁶ yielded results consistent with this exponential form, the work of Ref. 5 suggests that this is not the case. The discussion of Sec. III will clarify why these analyses arrived at different conclusions and confirm the exponentiation.

III. LARGE-MASS LEPTON PAIRS: ALL ORDERS

As an intermediate step to the all orders result consider two-gluon emission as in Fig. 6. Con-

TABLE I. Contributions to the integrand $I(\theta, \mu)$ of Eq. (2.15) from first-order diagrams.

Diagram	Feynman	Axial $n=p_1$	Axial $n=p_2$	Axial $n=p_1+p_2$	Planar $n=p_1+p_2$
	$\frac{\mu}{\theta}$ (1)	$\frac{\mu}{\theta}$ (1)	$\frac{\mu^2 - 2\mu + 2}{\theta\mu}$ (2)	$\frac{\mu}{\theta} + \frac{2(1-\mu)}{\theta(\theta+\mu)} - \frac{2}{(\theta+\mu)^2}$ (2)	$\frac{\mu}{\theta} + \frac{2(1-\mu)}{\theta(\theta+\mu)}$ (2)
	$\frac{\theta}{\mu}$ (1)	$\frac{\theta^2 - 2\theta + 2}{\theta\mu}$ (2)	$\frac{\theta}{\mu}$ (1)	$\frac{\theta}{\mu} + \frac{2(1-\theta)}{\mu(\theta-\mu)} - \frac{2}{(\theta+\mu)^2}$ (2)	$\frac{\theta}{\mu} + \frac{2(1-\theta)}{\mu(\theta+\mu)}$ (2)
	$\frac{1-\theta-\mu}{\theta\mu}$ (2)	$\frac{-1}{\mu}$ (1)	$\frac{-1}{\theta}$ (1)	$\frac{2(1-\theta-\mu)}{(\theta+\mu)^2}$ (1)	$\frac{-2}{\theta+\mu}$ (0)
	$\frac{1-\theta-\mu}{\theta\mu}$ (2)	$\frac{-1}{\mu}$ (1)	$\frac{-1}{\theta}$ (1)	$\frac{2(1-\theta-\mu)}{(\theta+\mu)^2}$ (1)	$\frac{-2}{\theta+\mu}$ (0)

Feynman Gauge: $d_{\mu\nu}(k) = -g_{\mu\nu}$

Axial gauge: $d_{\mu\nu}(k) = -g_{\mu\nu} + \frac{n_\mu k_\nu + n_\nu k_\mu}{n \cdot k} - n^2 \frac{k^\mu k^\nu}{(n \cdot k)^2}$

Planar gauge: $d_{\mu\nu}(k) = -g_{\mu\nu} + \frac{n_\mu k_\nu + n_\nu k_\mu}{n \cdot k}$

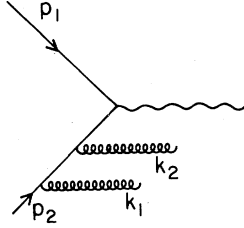


FIG. 6. Two-gluon emission from the same quark line.

considerable simplification is obtained by using the *planar gauge*,⁵ where the spin-summed gluon propagator is

$$D_{\mu\nu}(k) = \left(-g_{\mu\nu} + \frac{k_\mu n_\nu + k_\nu n_\mu}{n \cdot k} \right) \frac{1}{k^2} \quad (3.1a)$$

with

$$\begin{aligned} Q^2 \frac{d^2 \hat{\sigma}^{(2)}}{dQ^2 dQ_T^2} &\simeq \left(\frac{\alpha_s C_F}{2\pi} \right)^2 \hat{\sigma}_0 \int \frac{d^2 \vec{k}_{T1}}{\pi} d\mu_1 d\theta_1 \delta \left(\theta_1 \mu_1 - \frac{\vec{k}_{T1}^2}{\hat{s}} \right) \\ &\times \int \frac{d^2 \vec{k}_{T2}}{\pi} d\mu_2 d\theta_2 \delta \left(\theta_2 \mu_2 - \frac{\vec{k}_{T2}^2}{\hat{s}} \right) (-2\hat{s})^2 \pi \delta^{(2)}(\vec{k}_{T1} + \vec{k}_{T2} + \vec{Q}_T) \\ &\times \delta \left(1 - \theta_1 - \theta_2 - \mu_1 - \mu_2 + \mu_1 \theta_2 + \mu_2 \theta_1 - \frac{Q^2}{\hat{s}} \right) \frac{1}{2n \cdot k_1 2n \cdot k_2 D_1 D_2}, \end{aligned} \quad (3.3)$$

where terms with explicit factors of θ_i , μ_i , or \vec{k}_{Ti} in the numerator have been dropped. The various propagator factors are

$$2n \cdot k_i = \hat{s}(\theta_i + \mu_i), \quad (3.4a)$$

$$D_1 = (p_2 - k_1)^2 = -\hat{s}\mu_1, \quad (3.4b)$$

and

$$\begin{aligned} D_2 &= (p_2 - k_1 - k_2)^2 \\ &= -\hat{s} \left[\mu_1(1 - \theta_2) + \mu_2(1 - \theta_1) - \frac{\vec{k}_{T1} \cdot \vec{k}_{T2}}{\hat{s}} \right]. \end{aligned} \quad (3.4c)$$

The maximum number of logarithms comes from the kinematic region where both the θ_i and the μ_i are small. Hence, to DLLA the θ_i and μ_i can be set to zero in the argument of the $Q^2 \delta$ function and the upper limits of the θ_i integrals can all be set equal to 1. (Note that this simplification is possible only in planar and axial gauges, where the gauge denominator $\theta_i + \mu_i$ provides a cutoff as $\theta_i \rightarrow 0$ and the usual phase-space cutoff from the $Q^2 \delta$ function is redundant.) Furthermore, the maximum number of logarithms arise when the μ_i are ordered. In this case $\mu_1 < \mu_2$ and $D_2 \approx \hat{s}\mu_2$, where the $\vec{k}_{T1} \cdot \vec{k}_{T2}/\hat{s}$ term has also been dropped. Note that due to the mass-shell δ functions for each gluon

$$n = p_1 + p_2. \quad (3.1b)$$

In this case all the leading double logarithms come from the ladder-type diagrams, for example, the square of Fig. 6. More specifically, only the $1/n \cdot k$ piece of each gluon propagator gives a leading contribution. This structure ensures that the three-gluon coupling plays no role in DLLA. A further advantage of using the planar gauge is that interference diagrams, where a gluon couples a quark to an antiquark, are down by at least *two* powers of the logarithm, as shown in lowest order in Table I.

As before, parametrize the gluon momenta

$$k_i = \theta_i p_2 + \mu_i p_1 + \vec{k}_{Ti}. \quad (3.2)$$

After taking the trace in the square of Fig. 6 and canceling two propagators, one finds a leading contribution of the form

$$\mu_i = \frac{\vec{k}_{Ti}^2}{\hat{s}\theta_i}. \quad (3.5)$$

Hence the constraint

$$\frac{\vec{k}_{T1}^2}{\hat{s}\theta_1} < \frac{\vec{k}_{T2}^2}{\hat{s}\theta_2} \quad (3.6a)$$

yields ($\theta_1, \theta_2 < 1$)

$$\left| \frac{\vec{k}_{T1} \cdot \vec{k}_{T2}}{\hat{s}} \right| < \frac{\vec{k}_{T2}^2}{\hat{s}} \left(\frac{\theta_1}{\theta_2} \right)^{1/2} < \frac{\vec{k}_{T2}^2}{\hat{s}\theta_2}. \quad (3.6b)$$

The only remaining question is whether the \vec{k}_{Ti} themselves are ordered. If one were interested only in the collinear singularities, for example, in the calculation of the Q^2 dependence of the quark distribution functions, then one would treat the θ_i as all finite (i.e., not asymptotically small) and the ordering of the \vec{k}_{Ti} 's would follow from that of the μ_i 's. However, here the region of interest is for all θ_i vanishing and hence a more careful analysis is required. It turns out, in fact, that all orderings of the \vec{k}_{Ti} 's contribute to the leading double logarithms. To see this, write the leading-logarithm part of Eq. (3.3) as, after evaluating the μ_i integrals,

$$\frac{d^2\hat{\sigma}^{(2)}}{dQ^2 dQ_T^2} \underset{\text{DLLA}}{\simeq} \hat{\sigma}_0 \left(\frac{\alpha_s C_F}{2\pi} \right)^2 \delta(Q^2 - \hat{s}) \int \frac{d^2\vec{k}_{T1}}{\pi} \int d\theta_1 \frac{2}{\vec{k}_{T1}^2 [\theta_1 + (\vec{k}_{T1}^2/\theta_1 \hat{s})]} \\ \times \int \frac{d^2\vec{k}_{T2}}{\pi} \int d\theta_2 \frac{2}{\vec{k}_{T2}^2 [\theta_2 + (\vec{k}_{T2}^2/\theta_2 \hat{s})]} \pi \delta^{(2)}(\vec{k}_{T1} + \vec{k}_{T2} + \vec{Q}_T), \quad (3.7)$$

where the regions of integration are constrained to satisfy $\vec{k}_{T2}^2/\hat{s}\theta_2 > \vec{k}_{T1}^2/\hat{s}\theta_1$. Now consider the two possible \vec{k}_{Ti} orderings $\vec{k}_{T1}^2 < \vec{k}_{T2}^2 \sim Q_T^2$ and $\vec{k}_{T2}^2 < \vec{k}_{T1}^2 \sim Q_T^2$ which correspond to the transverse momentum of the virtual photon being balanced by the inner and outer gluons, respectively. In the first region relabel the variables as $\vec{k}_{T1} = \vec{l}_T$, $\theta_1 = x_1$, and $\theta_2 = x_2$. In the second region relabel $\vec{k}_{T2} = \vec{l}_T$, $\theta_2 = x_1$, and $\theta_1 = x_2$. The integral becomes, with the usual λ^2 infrared cutoff,

$$\frac{d^2\hat{\sigma}^{(2)}}{dQ^2 dQ_T^2} \underset{\text{DLLA}}{\simeq} \hat{\sigma}_0 \left(\frac{\alpha_s C_F}{2\pi} \right)^2 \delta(Q^2 - \hat{s}) \frac{1}{Q_T^2} \left\{ \int_0^1 dx_2 \frac{2}{x_2 + Q_T^2/\hat{s}x_2} \int_{\lambda^2}^{Q_T^2} \frac{dl_T^2}{l_T^2} \int_0^1 dx_1 \frac{2}{x_1 + l_T^2/\hat{s}x_1} \left[\frac{l_T^2 < Q_T^2}{\hat{s}x_1} \right] \right. \\ \left. + \int_0^1 dx_2 \frac{2}{x_2 + Q_T^2/\hat{s}x_2} \int_{\lambda^2}^{Q_T^2} \frac{dl_T^2}{l_T^2} \int_0^1 dx_1 \frac{2}{x_1 + l_T^2/\hat{s}x_2} \left[\frac{Q_T^2 < l_T^2}{\hat{s}x_2} \right] \right\}, \quad (3.8)$$

where the x_i integration regions are specified by the inequalities in the square brackets. Clearly the two \vec{k}_{Ti} orderings both make leading contributions, the first giving $\frac{1}{8} \ln(\hat{s}/Q_T^2) \ln^2(\hat{s}/\lambda^2) - \frac{1}{8} \ln^3(\hat{s}/Q_T^2)$ and the second $\frac{1}{8} \ln^3(\hat{s}/Q_T^2)$.

It is apparently at this point that the analysis of Ref. 5 differs from the present one and those of Ref. 6. While the structure of the calculation performed here is somewhat different from that of Ref. 5, the essential difference is that in Ref. 5 the assumption is made that $\vec{k}_{T2}^2 \sim Q_T^2$ always. Coupled with the μ_i ordering, $\vec{k}_{T1}^2/\theta_1 \leq \vec{k}_{T2}^2/\theta_2 \sim Q_T^2/\theta_2$, this leads to an integration over two regions in \vec{k}_{T1} and θ_1 space. The first is $1 > \theta_1 > \theta_2 \vec{k}_{T1}^2/Q_T^2$, $\lambda^2 < \vec{k}_{T1}^2 < Q_T^2$ which coincides with the first region in Eq. (3.8) and yields the contribution $\frac{1}{8} [\ln(\hat{s}/Q_T^2)] [\ln^2(\hat{s}/\lambda^2)] - \frac{1}{8} \ln^3(\hat{s}/Q_T^2)$. The second, different from the second region above, is $1 > \theta_1 > \theta_2 \vec{k}_{T1}^2/Q_T^2$ and $Q_T^2 < \vec{k}_{T1}^2 < Q_T^2/\theta_2 \leq (Q_T^2 \hat{s})^{1/2}$, using $\theta_2 \gtrsim (Q_T^2/\hat{s})^{1/2}$. This latter region yields a contribution $\frac{1}{8} \ln^3(\hat{s}/Q_T^2)$.

All analyses agree on the contribution of the diagram with one gluon emitted from the quark and one from the antiquark. There are two distinct, symmetric regions of integration, again corresponding to transverse-momentum balance by a single gluon, and the result is $\frac{1}{4} [\ln(\hat{s}/Q_T^2)] [\ln^2(\hat{s}/$

$\lambda^2)] - \frac{1}{4} \ln^3(\hat{s}/Q_T^2)$. Thus the sum of this last contribution plus two-gluon emission from the quark plus two-gluon emission from the antiquark gives $\frac{1}{2} \{ [\ln(\hat{s}/Q_T^2)] [\ln^2(\hat{s}/\lambda^2)] - \ln^3(\hat{s}/Q_T^2) \}$ in the present analysis and $\frac{1}{2} \{ [\ln(\hat{s}/Q_T^2)] [\ln^2(\hat{s}/\lambda^2)] - \frac{13}{12} \ln^3(\hat{s}/Q_T^2) \}$ in that of Ref. 5. (The factor $\frac{13}{12}$ is recognizable as the coefficient of $(1/2!) [(\alpha_s C_F/2\pi) \ln^2(\hat{s}/Q_T^2)]^2$ in the expansion of the T form factor of Ref. 5.) The difference comes from the second region discussed above where, since $\vec{k}_{T2}^2 \sim Q_T^2$ is always assumed, the reverse ordering of the \vec{k}_{Ti} 's leads to $\vec{k}_{T1}^2 > Q_T^2$ in violation of transverse-momentum conservation. A correct treatment based more on the structure and language of Ref. 5 is given in Ref. 7.

Returning to Eq. (3.8), it should be noted that not only do the two regions of integration yield comparable contributions, their union (after relabeling) spans the entire region of x_i space while the \vec{l}_T integral is "nested": $\lambda^2 < \vec{l}_T^2 < Q_T^2$. The result of summing over all \vec{k}_{Ti} orderings, with appropriate relabeling, is to replace the constraints of the μ_i ordering with nested \vec{l}_{Ti} integrals and unconstrained x_i integrals.

Consider now n -gluon emission in the ladder configuration of Fig. 7 (squared). In DLLA the general form is

$$Q^2 \frac{d^2\hat{\sigma}^{(n)}}{dQ^2 dQ_T^2} \simeq \hat{\sigma}_0 \prod_{i=1}^n \left[\int d\theta_i d\mu_i \frac{d^2\vec{k}_{Ti}}{\pi} \delta\left(\theta_i \mu_i - \frac{\vec{k}_{Ti}^2}{\hat{s}}\right) \frac{-C_F \alpha_s \hat{s}}{2\pi n \cdot k_i D_i} \right] \\ \times \pi \delta^{(2)}\left(\sum_{i=1}^n \vec{k}_{Ti} + \vec{Q}_T\right) \hat{s} \delta\left(Q^2 - \left(p_1 + p_2 - \sum_{i=1}^n k_i\right)^2\right). \quad (3.9)$$

Again focus only on $\mu_i, \theta_i \rightarrow 0$ and order the μ_i so that

$$D_i \simeq -\hat{s} \mu_i. \quad (3.10)$$

Once again the sum over *all* the $n!$ possible \vec{k}_{Ti} orderings, with appropriate relabeling of the variables,

will remove the apparent constraint on the θ_i due to the μ_i ordering. For example, if $\vec{k}_{T_{i_1}}^2 < \vec{k}_{T_{i_2}}^2 < \dots < \vec{k}_{T_{i_n}}^2 \sim Q_T^2$, then relabel $\vec{k}_{T_{i_r}}^2 = \vec{l}_{T_r}^2$ and $\theta_{i_r} = x_r$. Thus Eq. (3.9) becomes

$$Q^2 \frac{d^2 \hat{\sigma}^{(n)}}{dQ^2 dQ_T^2} \underset{\text{DLLA}}{\simeq} \hat{\sigma}_0 \left(\frac{\alpha_s C_F}{2\pi} \right)^n \frac{1}{Q_T^2} \int_0^1 dx_n \frac{2}{x_n + (Q_T^2/\hat{s}x_n)} \\ \times \int_{\lambda^2}^{<Q_T^2} \frac{d\vec{l}_{T_{n-1}}^2}{\vec{l}_{T_{n-1}}^2} \int_0^1 dx_{n-1} \frac{2}{x_{n-1} + (\vec{l}_{T_{n-1}}^2/\hat{s}x_{n-1})} \dots \\ \times \int_{\lambda^2}^{\vec{l}_{T_2}^2} \frac{d\vec{l}_{T_1}^2}{\vec{l}_{T_1}^2} \int_0^1 dx_1 \frac{2}{x_1 + (\vec{l}_{T_1}^2/\hat{s}x_1)} \delta \left(1 - \frac{Q^2}{\hat{s}} \right) \quad (3.11a)$$

$$\underset{\text{DLLA}}{\simeq} \hat{\sigma}_0 \delta \left(1 - \frac{Q^2}{\hat{s}} \right) \left(\frac{\alpha_s C_F}{2\pi} \right)^n \frac{\ln(\hat{s}/Q_T^2)}{Q_T^2} \frac{1}{(n-1)!} \left(\frac{1}{2} \ln^2 \frac{\hat{s}}{\lambda^2} - \frac{1}{2} \ln^2 \frac{\hat{s}}{Q_T^2} \right)^{n-1}, \quad (3.11b)$$

where the $1/(n-1)!$ arises from the nesting of the \vec{l}_{T_i} integrals. Alternatively, one could integrate over all \vec{l}_{T_i} symmetrically and simply divide by $(n-1)!$ to account for double counting as was done in the QED analysis of Ref. 9. Thus the result of summing to all orders the emission of gluons from a single quark line is

$$Q^2 \frac{d^2 \hat{\sigma}^{(\text{all})}}{dQ^2 dQ_T^2} \Big|_{\text{quark line}} \underset{\text{DLLA}}{\simeq} \hat{\sigma}_0 \delta \left(1 - \frac{Q^2}{\hat{s}} \right) \frac{\alpha_s C_F}{2\pi} \frac{\ln(\hat{s}/Q_T^2)}{Q_T^2} \left\{ \exp \left[\frac{\alpha_s C_F}{4\pi} \left(\ln^2 \frac{\hat{s}}{\lambda^2} - \ln^2 \frac{\hat{s}}{Q_T^2} \right) \right] \right\}. \quad (3.12)$$

When the emissions from the other quark line are included there are two changes. First, the exponent is doubled due to the contribution where Q_T is still balanced by a gluon from the lower quark line (i.e., the emissions from the upper line produce a second *factor* of the exponential) and, second, there is an overall factor of 2 from the symmetric contribution where Q_T is balanced by a gluon from the upper quark line. Finally, the inclusion of virtual-gluon corrections¹² gives an overall *factor* $\exp(-\alpha_s C_F/2\pi \ln^2 \hat{s}/\lambda^2)$ which cancels the λ^2 dependence, as was illustrated explicitly in lowest order. Hence, the final result is

$$Q^2 \frac{d^2 \hat{\sigma}}{dQ^2 dQ_T^2} \underset{\text{DLLA}}{\simeq} \hat{\sigma}_0 \delta \left(1 - \frac{Q^2}{\hat{s}} \right) \frac{\alpha_s C_F}{\pi} \frac{\ln(\hat{s}/Q_T^2)}{Q_T^2} \\ \times \exp \left(-\frac{\alpha_s C_F}{2\pi} \ln^2 \frac{\hat{s}}{Q_T^2} \right) \quad (3.13)$$

as previously suggested.⁶ In terms of the quantity

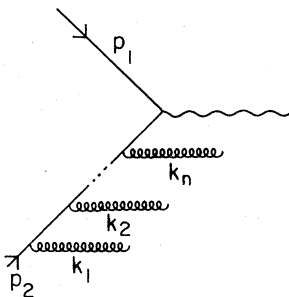


FIG. 7. n -gluon emission from the same quark line.

defined in Eq. (2.8),

$$\Sigma_n \left(\frac{p_T^2}{\hat{s}} \right) \underset{\text{DLLA}}{\simeq} \hat{\sigma}_0 \exp \left(-\frac{\alpha_s C_F}{2\pi} \ln^2 \frac{\hat{s}}{p_T^2} \right). \quad (3.14)$$

Note that, as in lowest order [Eq. (2.14b)], the DLLA result is independent of n and λ^2 . Although in DLLA one does not see the order $\alpha_s^m \ln^m p_T^2/\lambda^2$ structure-function logarithms explicitly, the above result is of course *consistent* with the factorized form

$$\Sigma_n \left(\frac{p_T^2}{s} \right) = T \left(\frac{p_T^2}{s} \right) \langle G_q(p_T^2) \rangle_n \langle G_{\bar{q}}(p_T^2) \rangle_n \quad (3.15)$$

suggested in Ref. 5 with a different form for T . Here $\langle G_q(p_T^2) \rangle_n$ is the n th moment of the quark structure function evaluated at scale p_T^2 , given by (α_s fixed, nonsinglet part only)

$$\langle G_q(p_T^2) \rangle_n \simeq \exp \left(a_n \frac{\alpha_s C_F}{2\pi} \ln \frac{p_T^2}{\lambda^2} \right). \quad (3.16)$$

Note that, for $Q_T^2 \leq p_T^2 \ll \hat{s} \leq s$, it is the transverse-momentum scale p_T^2 which controls the collinear logarithms and hence the nonscaling of the distribution functions. This was illustrated explicitly in lowest order in Eq. (2.14a).

In summary, the DLLA does lead to an *exponential* damping which receives contributions in perturbation theory from the region of phase space where the μ_i are ordered along the ladder. The transverse momenta of the gluons are also ordered in DLLA but *all* orderings contribute, i.e., there are leading contributions where each of the gluons balances the Q_T of the photon.

IV. BEYOND THE DLLA

Consider the expression in Eq. (3.13) as a function of Q_T^2 . It exhibits the interesting behavior of vanishing both as $Q_T^2 \rightarrow 0$ as Q_T^2 approaches \hat{s} . The intermediate peak occurs for

$$\ln \frac{\hat{s}}{Q_T^2} \Big|_{\text{peak}} = \frac{1 + [1 + (4\alpha_s C_F / \pi)]^{1/2}}{2\alpha_s C_F / \pi} \simeq \frac{\pi}{\alpha_s C_F} \equiv z_p, \quad (4.1)$$

where $\alpha_s \ll 1$ is assumed in the last step. It is clearly important to determine if such a peak is observable experimentally. The question also arises as to whether the DLLA is a satisfactory approximation in the region of the peak. Consider the expansion of the exponential near the peak in $z = \ln \hat{s} / Q_T^2$,

$$\exp\left(-\frac{\alpha_s C_F}{2\pi} z^2\right) = \sum_{n=0}^{\infty} \frac{(-1)^n}{n!} \left(\frac{\alpha_s C_F}{2\pi}\right)^n z^{2n} \\ \simeq_{z \approx z_p} \sum_{n=0}^{\infty} \frac{(-1)^n}{n!} \left(\frac{z_p}{2}\right)^n. \quad (4.2)$$

This latter series is dominated by terms around

$$n_{\max} \simeq \frac{z_p}{2} = \frac{\pi}{2\alpha_s C_F} \quad (4.3)$$

such that the n_{\max} th and $(n_{\max} + 1)$ th terms are comparable in magnitude. Now consider a next-to-leading contribution from the region of phase space where all the gluons are collinear but one is not soft. At order α_s^n there are precisely n choices of which gluon is not soft, and the contribution is of the form $n \alpha_s^n z^{2n-1}$. However, in the region of the peak $z \approx z_p$, and for $n \sim n_{\max}$ this term is of magnitude $(1/n!)^{1/2} (z_p/2)^n$, i.e., of the same order as the leading term. Next-to-leading logarithms can also arise from a more careful treatment of the scale in the running coupling constant of Eq. (1.1) which has been ignored (correctly) in DLLA. For example, $\alpha_s(p_T^2)$ can be reexpressed in terms of $\alpha_s(\hat{s})$ via

$$\alpha_s(p_T^2) = \frac{b}{\ln(p_T^2/\Lambda^2)} \\ \simeq \alpha_s(\hat{s}) \left[1 + \frac{\alpha_s(\hat{s})}{b} \ln \frac{\hat{s}}{p_T^2} + \dots \right] \quad (4.4)$$

and such a change in the argument of α_s will change the subleading terms. Hence the determination of the position and magnitude of the peak requires a treatment enlarged to include at least the next to double leading logarithms (NDLLA) arising from both the running coupling and the configuration where one gluon is not soft.

Contributions where one gluon is not soft arise from terms in the numerator (trace) which involve a single θ_i to some positive power. For n -gluon emission the inclusion of such contributions adds to Eq. (3.9) a factor $1 - \sum_{i=1}^n (\theta_i - \frac{1}{2}\theta_i^2)$. Again the leading contribution in $\ln \hat{s} / Q_T^2$ arises from the case of ordered μ_i and the sum of all permutations of the ordered k_{T_i} . The overall δ function is $\delta(\hat{s}(1 - \sum \theta_i) - Q^2)$ but this imposes no constraint on the θ_i integrals since only one θ_i is nonzero in NDLLA. The NDLLA contribution to the cross section can, therefore, be calculated using the same techniques as before. Notice, however, that the additional factor $1 - \sum_{i=1}^n (\theta_i - \frac{1}{2}\theta_i^2)$ is simply the leading two terms in the expansion of the usual nested kernels (Altarelli-Parisi functions¹¹) which yield the renormalization of the structure function in the leading-(collinear) logarithm approximation. In terms of more usual variables the iterated kernel is

$$K_n = \prod_{i=1}^n \left(\frac{1 - \alpha_i}{2} + \frac{\alpha_i}{1 - \alpha_i + \mu_i \prod_{j=0}^{i-1} \alpha_j^{-1}} \right), \quad (4.5)$$

where α_i is the ratio of the quark momentum after emission of gluon i to that before the emission, i.e., $\theta_i = (1 - \alpha_i) \prod_{j=0}^{i-1} \alpha_j$ and $\alpha_0 = 1$. In NDLLA the above kernel will give the same result as the factor $1 - \sum_i (\theta_i - \frac{1}{2}\theta_i^2)$. Thus with the substitution

$$\frac{1 - \sum_{i=1}^n (\theta_i - \frac{1}{2}\theta_i^2)}{\prod_{i=1}^n (\theta_i + \mu_i)} \rightarrow K_n, \quad (4.6)$$

Eq. (3.9) becomes

$$\frac{d^2 \hat{\sigma}^{(n)}}{dQ^2 dQ_T^2} \Big|_{\text{NDLLA}} \simeq \hat{\sigma}_0 \prod_{i=1}^n \left[\int d\theta_i d\mu_i \frac{d^2 \vec{k}_{T_i}}{\pi} \delta\left(\theta_i \mu_i - \frac{\vec{k}_{T_i}^2}{\hat{s}}\right) \frac{\alpha_s C_F}{\pi D_i} K_n \right. \\ \left. \times \pi \delta^{(2)}\left(\sum_{j=1}^n \vec{k}_{T_j} + \vec{Q}_T\right) \delta\left(\left(p_1 + p_2 - \sum_{k=1}^n k_k\right)^2 - Q^2\right) \right]. \quad (4.7)$$

As before, the dominant contribution comes from ordered μ_i 's and all permutations of k_{T_i} 's, and the result is

$$\frac{d^2\hat{\sigma}^{(n)}}{dQ^2 dQ_T^2} \underset{\text{NDLLA}}{\simeq} \hat{\sigma}_0 \frac{C_F \alpha_s}{2\pi Q_T^2} \int_0^1 d\alpha_n \frac{1 + \alpha_n^2}{1 - \alpha_n + [Q_T^2/\hat{s}(1 - \alpha_n)]} \times \prod_{i=1}^{n-1} \left| \int_{\lambda^2}^{l_{T_{i+1}}^2} \frac{dl_{T_i}^2}{l_{T_i}^2} \int_0^1 d\alpha_i \frac{C_F \alpha_s}{2\pi} \frac{1 + \alpha_i^2}{1 - \alpha_i + [l_{T_i}^2/\hat{s}(1 - \alpha_i)]} \right| \delta\left(\hat{s} \prod_{j=1}^n \alpha_j - Q^2\right). \quad (4.8)$$

It is important to note that the expressions in Eqs. (4.7) and (4.8) are equal *only* in NDLLA. For example, the $\prod \alpha_i$ terms which appear in the denominators in K_n have been dropped in going from Eq. (4.7) to Eq. (4.8). However, it can be shown that the inclusion of such terms results in a loss of at least *two* logarithms.

In the calculation of the Q^2 dependence of structure functions, running coupling effects are correctly taken into account by replacing α_s by $\alpha_s(\vec{k}_{T_i}^2)$ in each gluon phase-space integral. However, since in this case the θ_i are all finite, to leading order it is immaterial whether the argument of α_s is $\vec{k}_{T_i}^2$ or $\mu_i \hat{s} = \vec{k}_{T_i}^2/\theta_i$. The net effect is to soften the integrals from log to log log and $\alpha_s \log Q^2$ is replaced by $\log[1/\alpha_s(Q^2)]$ in the result. In the present context, the θ_i are asymptotically small in DLLA and the next-to-leading corrections depend sensitively on the choice of the argument of α_s . It has been shown¹³ that in fact $\alpha_s(\vec{k}_{T_i}^2)$ rather than $\alpha_s(\vec{k}_{T_i}^2/\theta_i)$ is the correct choice, the substitution effectively replacing $\alpha_s \log^2 Q^2$ by $(\log Q^2)\{\log[1/\alpha_s(Q^2)]\}$ in the result.

The final NDLLA modification, therefore, is to replace α_s by $\alpha_s(\vec{l}_{T_i}^2)$ in Eq. (4.8). The iterated kernel is then given by [$b = 12\pi/33 - 2N_f$, as in Eq. (1.1)]

$$\frac{bC_F}{2\pi} \int_{\lambda^2}^{k_T^2} \frac{dl_T^2}{l_T^2 \ln(l_T^2/\Lambda^2)} \int_0^1 d\alpha \frac{1 + \alpha^2}{1 - \alpha + l_T^2/\hat{s}(1 - \alpha)} \underset{\text{NDLLA}}{\simeq} -\frac{bC_F}{2\pi} \left\{ \left[\ln\left(\frac{\ln(k_T^2/\Lambda^2)}{\ln(\lambda^2/\Lambda^2)}\right) \right] \left(\ln \frac{\hat{s}}{\Lambda^2} - \frac{3}{2} \right) - \ln \frac{k_T^2}{\lambda^2} \right\}. \quad (4.9)$$

Hence when all ladders and virtual contributions are summed the result is [c.f. Eq. (3.14)]

$$\Sigma_n\left(\frac{p_T^2}{\hat{s}}, \frac{\lambda^2}{\hat{s}}\right) \underset{\text{NDLLA}}{\simeq} \Sigma_0\left(\frac{p_T^2}{\hat{s}}\right) M_n(p_T^2) \bar{M}_n(p_T^2), \quad (4.10)$$

where

$$\Sigma_0\left(\frac{p_T^2}{\hat{s}}\right) = \hat{\sigma}_0 \exp\left(\frac{-bC_F}{\pi} \left\{ \left[\ln\left(\frac{\ln(\hat{s}/\Lambda^2)}{\ln(p_T^2/\Lambda^2)}\right) \right] \left(\ln \frac{\hat{s}}{\Lambda^2} - \frac{3}{2} \right) - \ln \frac{\hat{s}}{p_T^2} \right\}\right) \quad (4.11)$$

and $M_n(p_T^2)$ is the n th moment of the nonsinglet quark distribution in a quark measured at scale

p_T^2 , i.e.,

$$M_n(p_T^2) = \exp\left[\frac{bC_F}{2\pi} \alpha_n \ln\left(\frac{\ln(p_T^2/\Lambda^2)}{\ln(\lambda^2/\Lambda^2)}\right)\right]. \quad (4.12)$$

Note that this result agrees with the $O(\alpha_s)$ calculation of Sec. II [Eq. (2.14a)] and the DLLA result of Sec. III [Eq. (3.14)]. It also has the same factorization properties as the Dokshitzer-Dyakonov-Troyan formula of Ref. 5, i.e., the cross section is a convolution of quark structure functions with an overall T form factor given by Eq. (4.11). Again note that the scale p_T^2 controls the collinear singularities which yield the nonscaling distributions implicit in Eq. (4.12).

Recall that, when both the argument and the exponential are expanded, the result is correct for terms of order $[\ln(\hat{s}/\Lambda^2)]^{-n} [\ln(\hat{s}/p_T^2)]^{2n}$ and $[\ln(\hat{s}/\Lambda^2)]^{-n} [\ln(\hat{s}/p_T^2)]^{2n-1}$. The expression in Eq. (4.10) is presumed to correctly include all even "less-leading" logarithms of \hat{s}/p_T^2 which arise from all numbers of nonsoft but still collinear gluons, since the complete collinear kernel of Eq. (4.5) has been used. However, it certainly does not include contributions from situations where at least one gluon is not collinear. While it is, in principle, possible for such configurations to contribute at order $[\ln(\hat{s}/\Lambda^2)]^{-n} [\ln(\hat{s}/p_T^2)]^{2n-1}$ there is a cancellation (confirmed explicitly for $n=2$) between crossed and uncrossed ladders ensuring a leading contribution from such configurations only at order $[\ln(\hat{s}/\Lambda^2)]^{-n} [\ln(\hat{s}/p_T^2)]^{2n-2}$. At this level of accuracy interference diagrams where a gluon connects the quark and antiquark lines can also contribute. Furthermore, there are additional corrections to the behavior of α_s at this order. Hence it does not seem fruitful to pursue this sort of analysis beyond the next-to-leading-double-logarithm approximation. Further corrections will have only a small effect near the peak while inside the peak nonperturbative contributions are probably the dominant effect and outside the peak ordinary low-order perturbation theory rapidly becomes relevant. These essentially phenomenological questions are treated in more detail in the next section.

Another technique, which has been suggested¹⁴ as a means to enlarge the region of k_{T_i} space which is correctly included in the factorizing and, therefore, exponentiating form, is to represent the transverse-momentum-conserving δ function as an integral in impact-parameter space:

$$\delta\left(\vec{p}_T - \sum_i \vec{k}_{T_i}\right) = \int d^2b \exp\left[i\vec{b} \cdot \left(\vec{p}_T - \sum_i \vec{k}_{T_i}\right)\right]. \quad (4.13)$$

In this way the ordering of the k_{T_i} and the bound $k_{T_i} \lesssim p_T$ is replaced by the simple bound $k_{T_i} \ll (\hat{s})^{1/2}$ in order to maintain factorization. This region of momentum space then yields the correct Fourier-transformed quark form factor for $b \gg 1/(\hat{s})^{1/2}$ where the expression is damped as $\exp(-\ln^2 b^2 \hat{s})$ (the DLLA in b space). This implies that when the transform is inverted to obtain the form factor in p_T space the major contribution arises from small $b \lesssim 1/(\hat{s})^{1/2}$. This in turn requires a correct treatment of all of the k_{T_i} space including regions where dominance of the ladder graphs and simple factorization properties presumably do not hold. Hence, without a better understanding of the corrections to the small- b behavior arising from the regions of k_{T_i} space not treated correctly by the simple, factorizing expression, it is not at all clear that this procedure yields a better description of the true result compared to the direct momentum-space procedure discussed above, at least for $\Lambda \ll p_T \ll (\hat{s})^{1/2}$.

V. PHENOMENOLOGY

It is important now to consider whether the structure discussed in the previous sections is actually observable in experimental measurements. Note that its form is characteristic of the underlying field theory: the presence of logarithms squared is characteristic of a *vector*-boson theory while the form of the running coupling constant and the constants C_F and b are characteristic of a non-Abelian theory and, in particular, SU(3).

The quantity to be considered is essentially a quark form factor which is a function of two large kinematic variables, say p_T^2 and s , which satisfy $\Lambda^2 \ll p_T^2 \ll s$. Define the dimensionless variables

$$\eta = p_T^2/s, \quad (5.1a)$$

$$\xi = \ln(s/\Lambda^2), \quad (5.1b)$$

and

$$r = (1/\xi) \ln(1/\eta), \quad (5.1c)$$

which imply, for example,

$$p_T^2 = (\Lambda^2/s)^r. \quad (5.1d)$$

In terms of these variables the relevant regions are (i) $\eta \approx 1$, $r \rightarrow 0$ where there is really only one large variable, $\ln \eta \approx 0$, and usual lowest-order perturbation theory is appropriate, (ii) $\eta \lesssim \Lambda^2/s$, $r \gtrsim 1$ where perturbation theory in $\alpha_s(p_T^2)$ is inappropriate and nonperturbative effects due to the transverse momentum of quarks within hadrons

are important, (iii) $\Lambda^2 \ll p_T^2 \ll s$, $0 < r < 1$ where the present DLLA and NDLLA are presumably relevant. Now define an effective quark form factor, which is a function of these variables, by

$$F(p_T^2, s) = F(\eta, \xi) = \frac{1}{\sigma_0} \Sigma_0 \left(\frac{p_T^2}{s}, \frac{\Lambda^2}{s} \right). \quad (5.2)$$

Thus in NDLLA, Eq. (4.11) gives

$$F_1(\eta, \xi) \equiv \exp \left\{ -2\gamma \left[\left(\xi - \frac{3}{2} \right) \ln \left(\frac{\xi}{\xi + \ln \eta} \right) + \ln \eta \right] \right\} \quad (5.3a)$$

$$= \exp \left\{ -2\gamma \left[\left(\xi - \frac{3}{2} \right) \ln \frac{1}{1-r} - r\xi \right] \right\}, \quad (5.3b)$$

where

$$\gamma = \frac{bC_F}{2\pi} = \frac{6C_F}{33 - 2N_F} = \frac{8}{25} \quad (5.4)$$

for SU(3) and $N_F = 4$.

For purposes of comparison consider also the purely leading-double-logarithm result with $\alpha_s = b/\xi$:

$$F_2(\eta, \xi) \equiv \exp \left(-\gamma \frac{\ln^2 \eta}{\xi} \right) \quad (5.5a)$$

$$= \exp(-\gamma r^2 \xi) \quad (5.5b)$$

and the form which arises if only the corrections to the DLLA due to the running coupling are kept as

$$F_3(\eta, \xi) \equiv \exp \left\{ -2\gamma \left[\xi \ln \left(\frac{\xi}{\xi + \ln \eta} \right) + \ln \eta \right] \right\} \quad (5.6a)$$

$$= \exp \left[-2\gamma \left(\xi \ln \frac{1}{1-r} - r\xi \right) \right]. \quad (5.6b)$$

The quantity which exhibits the peaking behavior

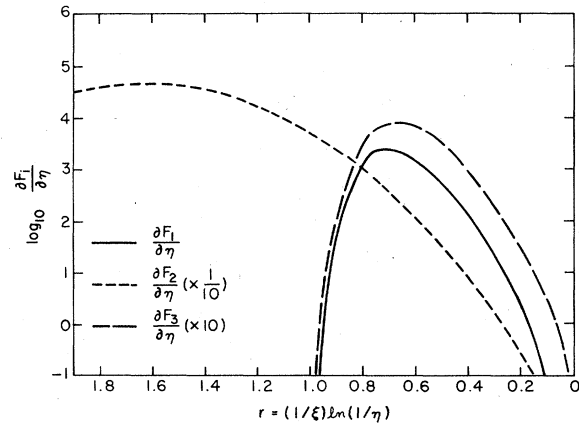


FIG. 8. The differential form factors $\partial F_i/\partial\eta$ defined in the text as a function of $r = (1/\xi) \ln(1/\eta)$. The curves correspond to $\sqrt{s} = 2 \times 10^3$ GeV and $\Lambda = 0.5$ GeV. For clarity, the values of $\partial F_2/\partial\eta$ have been divided by a factor of 10 and those of $\partial F_3/\partial\eta$ have been multiplied by a factor of 10.

discussed above is then $\partial F/\partial\eta$. Thus by operating on each of the F_i with $\partial/\partial\eta$ it is straightforward to study how the peaking behavior of this quantity is different in the various approximations. The location of the peak in η is given by the location of one of the solutions of

$$\left. \frac{\partial^2 F_i}{\partial\eta^2} \right|_{\eta_i^p = r_i^p \xi} = 0. \quad (5.7)$$

The appropriate solutions are

$$\begin{aligned} r_1^p &= \frac{1}{2\xi(1+2\gamma)} \left\{ \xi + \frac{3}{2}(1+4\gamma) \right. \\ &\quad \left. + [(\xi + \frac{3}{2} + 6\gamma)^2 - (1+2\gamma)(2\xi + 6 + 18\gamma)]^{1/2} \right\} \\ &\approx \frac{1}{1+2\gamma} + \frac{1}{\xi} \frac{(1+5\gamma)}{(1+2\gamma)} + \dots, \end{aligned} \quad (5.8a)$$

$$\begin{aligned} r_2^p &= \frac{1}{4\gamma\xi} [\xi + (\xi^2 + 8\gamma\xi)^{1/2}] \\ &\approx \frac{1}{2\gamma} + \frac{1}{\xi} + \dots, \end{aligned} \quad (5.8b)$$

$$\begin{aligned} r_3^p &= \frac{1}{2\xi(1+2\gamma)} \left\{ \xi + [\xi^2 + 4\xi(1+2\gamma)]^{1/2} \right\} \\ &\approx \frac{1}{1+2\gamma} + \frac{1}{\xi} + \dots. \end{aligned} \quad (5.8c)$$

Note, in particular, that the purely DLLA form factor F_2 has its peak at $r^p \approx 1/2\gamma > 1$ inside the non-perturbative region. However, the effect of including the running-coupling corrections, as in F_3 , and, even more, the rest of the next-to-leading double logarithms, as in F_1 , is to move the peak into the physically observable region at $r^p \approx 1/(1+2\gamma) < 1$. The magnitude of the peak is also influenced by these next-to-leading corrections as illustrated in Fig. 8 where the three curves $\partial F_i/\partial\eta$ are plotted. These comparisons are explicit illustrations of the points made in the discussion at the beginning of the last section.

Finally consider the crucial question of whether this peak can be seen experimentally. The signature is particularly striking as other effects, for example, nonperturbative transverse-momenta smearing, yield a broad peak at $Q_T=0$ and no peak at $Q_T>0$. As long as $r^p < 1$, as it is for all but the DLLA alone, then it is in principle possible to go to sufficiently large s that $Q_T \ll (s)^{1/2}$ and $Q_T^p \gg \Lambda$, $\langle k_T \rangle$, the characteristic quark transverse momentum in hadrons which would otherwise obscure the peak. Analyses¹⁵ of various types of data suggest that $\langle k_T^2 \rangle$ is in the range 0.3 to 1 (GeV/c)². Unfortunately, present data¹⁶ on large-mass lepton-pair production are primarily at Q^2 less than 50 GeV² with Q_T^p inside the region of effective smear-

ing.

Consider instead e^+e^- annihilation where data¹⁷ are now becoming available with Q^2 nearly 10³ GeV². Note also that in this case the relevant smearing arises from the average $\langle k_T^2 \rangle$ of hadrons within "jets" which is more like 0.1 to 0.3 (GeV/c)². The perturbative analysis of e^+e^- annihilation is virtually identical to that for lepton-pair production except that the quarks are now outgoing and the leptons incoming. The analogs of the moments Σ_n are quite naturally the energy-weighted cross sections⁸ or "antenna patterns" of hadronic energy flow. Like the lowest moment Σ_0 , these energy-weighted cross sections are independent of the details of the final process of fragmentation into hadrons as energy is still conserved.

Consider then the energy-energy correlation function⁸ defined in terms of the product of the energies, dE and dE' , which flow into two angular regions $d\Omega$ and $d\Omega'$ normalized to the total e^+e^- energy $W (= \sqrt{s})$. Thus

$$\frac{d^2\Sigma}{d\Omega d\Omega'} = \frac{\sum_{\text{events}} (dE dE')}{\mathcal{L} T W^2 d\Omega d\Omega'}, \quad (5.9)$$

where \mathcal{L} is the luminosity and T is the time of data taking. The normalization is

$$\int d\Omega d\Omega' \frac{d^2\Sigma}{d\Omega d\Omega'} = \sigma_{\text{tot}}. \quad (5.10)$$

For the case of two calorimeters which are nearly back to back such that

$$\cos\chi = d\hat{\Omega} \cdot d\hat{\Omega}' \quad (5.11)$$

is near -1 . One finds¹⁸ the expression

$$\frac{d^2\Sigma}{d\Omega d\Omega'} \approx \frac{1}{8\pi} \frac{\partial}{\partial\eta} F \left(\eta = \frac{1 + \cos\chi}{2}, \xi = \ln \frac{W^2}{\Lambda^2} \right) \frac{d\sigma}{d\Omega^2}, \quad (5.12)$$

where

$$\frac{d\sigma}{d\Omega} = \frac{\alpha^2}{4W^2} \sum_f 3Q_f^2 (1 + \cos^2\theta) \quad (5.13)$$

with Q_f the electric charge of quark flavor f . Integrating over the external variables gives

$$\left. \frac{1}{\sigma_{\text{tot}}} \frac{d\Sigma}{d\cos\chi} \right|_{\cos\chi \approx -1} \approx \frac{1}{4} \frac{\partial}{\partial\eta} F \left(\eta = \frac{1 + \cos\chi}{2}, \xi = \ln \frac{W^2}{\Lambda^2} \right) \quad (5.14)$$

with normalization ($d\eta = \frac{1}{2} d\cos\chi$)

$$\frac{1}{\sigma_{\text{tot}}} \int_{\cos\chi \approx -1} d\cos\chi \frac{d\Sigma}{d\cos\chi} \approx \frac{1}{2} \quad (5.15)$$

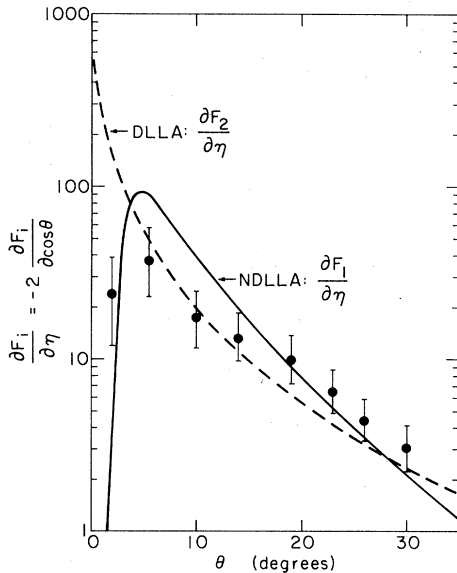


FIG. 9. Comparison of the energy-weighted cross section in DLLA (dashed line) and NDLLA (full line) with data from the PLUTO collaboration (Ref. 17). The curves correspond to $W = 30$ GeV, $\Lambda = 0.5$ GeV, and $N_f = 4$. Note that the peak in the DLLA curve is at $\theta = 0.12^\circ$.

as is appropriate for the contribution from one of the two jets in the final state. For $W = 30$ GeV, $\partial F_1/\partial \eta$ exhibits a peak near $(\pi - \chi) \sim 5^\circ$ for $\Lambda = 0.5$ GeV, which in turn corresponds to φ_T values near 1.3 GeV/c. The data from PLUTO¹⁷ have been treated slightly differently from the fashion suggested by Eqs. (5.14) and (5.15) but a comparison¹⁹ can be made for small values of $\theta = \pi - \chi$ as long as the normalization is 1 in Eq. (5.15) instead of $\frac{1}{2}$. Thus, in Fig. 9 the renormalized data are compared to $\partial F_i/\partial \eta$. Note, in particular, the suggestion of a damping in the smallest-angle bin and the general agreement in magnitude with F_1 . (The fit can be improved by decreasing the value of Λ slightly.) This is clearly an interesting question which deserves and presumably will receive further experimental study.

VI. CONCLUSIONS

In the context of perturbative QCD corrections to the parton model, soft- and collinear-gluon emissions summed to all orders generate an effective quark form factor which damps such processes in the limit when the hard-quark scattering occurs at small angles or small transverse momentum. This structure is in direct analogy to what occurs in QED. The double-logarithmic form is characteristic of vector-boson emission while the coefficients are characteristic of QCD. The result, in the double-leading-logarithm approximation, was shown explicitly to exponentiate. Contributions to the leading behavior arise from all kinematic orderings of the transverse momenta of the emitted gluons.

It was demonstrated that to satisfactorily discuss this damping in kinematic regions which are likely to be experimentally accessible, one must go beyond DLLA. The next-to-leading double logarithms resulting from one of the gluons not being soft were also shown to exponentiate. At least to order α_s^2 , these are the only next-to-leading contributions other than those arising from the running coupling constant which are also included in the final answer. This level of approximation appears to be the limit at which all order calculations are practical and seems to be sufficient to perform adequate phenomenological studies.

Preliminary studies of existing data suggest that such damping will not be seen for some time in hadronic lepton-pair production but may already have been observed in e^+e^- annihilation. Indeed it seems likely that a fairly thorough experimental analysis of the quark form factor via this latter process will be possible in the very near future.

ACKNOWLEDGMENTS

It is a pleasure to thank J. Bjorken, L. Brown, N. Fleishon, J. Ralston, D. Soper, J. Sullivan, and S. Wolfram for helpful conversations. This research was supported in part by the U. S. Department of Energy.

¹R. P. Feynman, *Photon-Hadron Interactions* (Benjamin, New York, 1972).

²D. Amati, R. Petronzio, and G. Veneziano, Nucl. Phys. B140, 54 (1978); B146, 29 (1978); R. K. Ellis, H. Georgi, M. Machacek, H. D. Politzer, and G. G. Ross, Nucl. Phys. B152, 285 (1979); S. B. Libby and G. Sterman, Phys. Rev. D 19, 2468 (1979).

³W. Marciano and H. Pagels, Phys. Rep. 36C, 137 (1978).

⁴See for example A. J. Buras, Rev. Mod. Phys. 52, 199 (1980).

⁵Yu. L. Dokshitzer, D. I. Dyakonov, and S. I. Troyan, Phys. Lett. 78B, 290 (1978); 79B, 269 (1978); Proceedings of the XIIIth Winter School of LNPI, Leningrad, 1978 (unpublished) [Report No. SLAC-TRANS-183, 1978 (unpublished)]; Phys. Rep. 58, 269 (1980). This reference contains a footnote which acknowledges an error in the derivation of the form factor.

⁶C. L. Basham, L. S. Brown, S. D. Ellis, and S. T. Love, Phys. Lett. 85B, 297 (1979); G. C. Fox and S. Wolfram, Caltech Report No. CALT 68-723, 1979 (unpublished); C. Y. Lo and J. D. Sullivan, Phys. Lett. 86B, 327

- (1979); G. Parisi and R. Petronzio, Nucl. Phys. B154, 427 (1979); A. V. Smilga, Phys. Lett. 83B, 357 (1979). See also the earlier work of C. P. Korthals-Altes and E. De Rafael, Nucl. Phys. B106, 451 (1976); B125, 275, R. Coquereaux and E. De Rafael, Phys. Lett. 69B, 181 (1977).
- ⁷D. E. Soper, University of Oregon Report No. OITS-134, 1980 (unpublished).
- ⁸C. L. Basham, L. S. Brown, S. D. Ellis, and S. T. Love, Phys. Rev. D 17, 2298 (1978); Phys. Rev. Lett. 41, 1585 (1978); Phys. Rev. D 19, 2018 (1979).
- ⁹D. R. Yennie, S. C. Frautschi, and H. Suura, Ann. Phys. (N.Y.) 13, 379 (1961).
- ¹⁰G. T. Bodwin, C. Y. Lo, J. D. Stack, and J. D. Sullivan, Phys. Lett. 92B, 337 (1980).
- ¹¹G. Altarelli and G. Parisi, Nucl. Phys. B126, 298 (1977).
- ¹²V. V. Sudakov, Zh. Eksp. Teor. Fiz. 30, 87 (1956) [Sov. Phys.-JETP 3, 65 (1956)]; J. J. Carazzone, E. C. Poggio, and H. R. Quinn, Phys. Rev. D 11, 2286 (1975); J. M. Cornwall and G. Tiktopoulos, *ibid.* 13, 3370 (1976).
- ¹³S. J. Brodsky, SLAC Report No. SLAC-PUB-2447, 1979 (unpublished); Yu. L. Dokshitzer, D. I. Dyakonov, and S. I. Troyan, Ref. 5; A. B. Carter and C. H. Llewellyn Smith, Nucl. Phys. B163, 93 (1980).
- ¹⁴See, e.g., the fourth paper in Ref. 6.
- ¹⁵G. Altarelli, G. Parisi, and R. Petronzio, Phys. Lett. 76B, 351 (1978); 76B, 356 (1978); R. P. Feynman, R. D. Field, and G. C. Fox, Phys. Rev. D 18, 3320 (1978).
- ¹⁶See, for example, C. Kourkomelis *et al.*, Phys. Lett. 91B, 475 (1980).
- ¹⁷PLUTO collaboration, Ch. Berger *et al.*, Phys. Lett. 90B, 312 (1980).
- ¹⁸See the first paper in Ref. 6.
- ¹⁹See, also, F. Halzen and D. M. Scott, University of Wisconsin Report No. UW-COO-881-130, 1980 (unpublished).